

Research Paper

Comparison of Oxidative Stress Effects on Senescence Patterning of Human Adult and Perinatal Tissue-Derived Stem Cells in Short and Long-term Cultures

Federica Facchin^{1,2*}, Eva Bianconi^{1,2*}, Miriam Romano¹, Alessia Impellizzeri¹, Francesco Alviano¹, Margherita Maioli^{3,4}, Silvia Canaider^{1,2✉} and Carlo Ventura^{1,2}

1. Department of Experimental, Diagnostic and Specialty Medicine (DIMES), University of Bologna, Via Massarenti 9, 40138 Bologna, Italy;
2. National Laboratory of Molecular Biology and Stem Cell Bioengineering of the National Institute of Biostructures and Biosystems (NIBB) – Eldor Lab, at the Innovation Accelerator, CNR, Via Piero Gobetti 101, 40129 Bologna, Italy;
3. Department of Biomedical Sciences, University of Sassari, Viale San Pietro 43/B, 07100 Sassari, Italy;
4. Istituto di Ricerca Genetica e Biomedica, Consiglio Nazionale delle Ricerche (CNR), Monserrato, 09042 Cagliari, Italy.

*These Authors equally contributed to this work

✉ Corresponding author: Silvia Canaider (Department of Experimental, Diagnostic and Specialty Medicine -DIMES, University of Bologna, Via Massarenti 9, 40138 Bologna, Italy, Tel: +39-051-2094104, Fax: +39-051-2094110 or E-mail address: silvia.canaider@unibo.it)

© Ivyspring International Publisher. This is an open access article distributed under the terms of the Creative Commons Attribution (CC BY-NC) license (<https://creativecommons.org/licenses/by-nc/4.0/>). See <http://ivyspring.com/terms> for full terms and conditions.

Received: 2018.05.09; Accepted: 2018.08.27; Published: 2018.10.20

Abstract

Human Mesenchymal Stem Cells (hMSCs) undergo senescence in lifespan. In most clinical trials, hMSCs experience long-term expansion *ex vivo* to increase cell number prior to transplantation, which unfortunately leads to cell senescence, hampering post-transplant outcomes.

Hydrogen peroxide (H₂O₂) *in vitro* represents a rapid, time and cost-effective tool, commonly used as oxidative stress tantalizing the stem cell ability to cope with a hostile environment, recapitulating the onset and progression of cellular senescence.

Here, H₂O₂ at different concentrations (ranging from 50 to 400 μM) and time exposures (1 or 2 hours - h), was used for the first time to compare the behavior of human Adipose tissue-derived Stem Cells (hASCs) and human Wharton's Jelly-derived MSCs (hWJ-MSCs), as representative of adult and perinatal tissue-derived stem cells, respectively. We showed timely different responses of hASCs and hWJ-MSCs at low and high subculture passages, concerning the cell proliferation, the cell senescence-associated β-Galactosidase activity, the capability of these cells to undergo passages, the morphological changes and the gene expression of *tumor protein p53* (*TP53*, alias *p53*) and *cyclin dependent kinase inhibitor 1A* (*CDKN1A*, alias *p21*) post H₂O₂ treatments.

The comparison between the hASC and hWJ-MSC response to oxidative stress induced by H₂O₂ is a useful tool to assess the biological mechanisms at the basis of hMSC senescence, but it could also provide two models amenable to test *in vitro* putative anti-senescence modulators and develop anti-senescence strategies.

Key words: human mesenchymal stem cells; cell senescence; oxidative stress-induced premature senescence; hydrogen peroxide; Resazurin-based assay; senescence-associated β-galactosidase activity

Introduction

The human body continuously repairs damaged tissues and opposes senescence-related processes due to the peculiar properties of its resident stem cells. Human mesenchymal stem cells (hMSCs) in fact are able of self-renewal and multi-lineage differentiation

and the equilibrium between these two events determines the stem cell fate and their roles in the human body [1]. They can be isolated and expanded *in vitro* from virtually all adult tissues [2], including bone marrow [3], adipose tissue [4], peripheral blood

[3], and also from several fetal and perinatal sources, as well as placenta [5], umbilical cord [6] and cord blood [7]. MSCs obtained from various sources differ in their biological characteristics [8,9], and their proteome and transcriptome profiles revealed source specific markers [10]. Moreover, diversity in multi-lineage differentiation potency and paracrine functions [8,9,11,12] determine different clinical applications of hMSCs [13]. Recently, hMSCs have been utilized for cell-based therapy in regenerative medicine to treat several injury and degenerative disorders, like Crohn's disease, diabetes mellitus, multiple sclerosis, myocardial infarction, liver failure, and rejection after liver transplant [14-21].

Since cell-based therapy procedures usually require hundreds of million hMSCs for each treatment (<http://www.clinicaltrials.gov>), cells isolated from donors need to be expanded *ex vivo* for several culture passages to obtain a large amount of cells prior to transplantation [13,22].

Unfortunately, as the function of hMSCs decreases with age *in vivo* [23,24], hMSCs, as well as all cultured primary cells [25], undergo cellular senescence along culture passages, with substantial decay in differentiation and self-renewal potential [22-24]. Premature senescence is a continuous process where cells share many molecular and functional characteristics, including changes in morphology, enhanced Senescence-Associated β -Galactosidase (SA β -Gal) activity, and permanent cell cycle arrest [22,26].

Oxidative stress, defined as an imbalance between the production of free radicals/Reactive Oxygen Species (ROS), and antioxidants [27], is thought to contribute significantly to DNA damage and cellular senescence [28-30]. According to the free radical or oxidative stress theory of aging [31], oxidative stress incurs when the cellular antioxidant defense systems fail to counteract ROS bringing them back to their basal levels.

For this reason, hydrogen peroxide (H_2O_2) treatment is commonly used as a model for assessing cellular susceptibility to oxidative stress. Although hMSCs appear to efficiently handle oxidative stress, nevertheless they undergo premature senescence *in vitro* when exposed to H_2O_2 [32,33]. Understanding hMSC behavior in oxidative stress would be important to study how to postpone, anticipate or revert Oxidative Stress-Induced Premature Senescence (OSIPS) in hMSC cultures.

It has been recently shown that OSIPS is a common feature in bone marrow hMSCs, the stem cell population that has been first isolated and characterized, with evidence ranging from morphological traits and SA β -Gal positivity to differential proteomic/metabolomic signatures in

H_2O_2 exposed cells, as compared with untreated controls [34-37]. In hMSCs isolated from adipose tissue (hASCs), H_2O_2 was found to increase intracellular ROS production and to reduce antioxidant defenses (*i.e.* superoxide dismutase - SOD and glutathione synthetase - GSH) [38], hampering cell viability in a dose- and exposure time- dependent manner [38,39]. It has been recently shown that SOD2 overexpression in ASCs promotes cell resistance to oxidative stress [40]. Moreover, H_2O_2 treatment provokes DNA breaks [41], raises SA β -Gal positive cells [42], alters the expression of senescent marker genes, as well as *p53*, *p21*, *mitogen-activated protein kinase 14* (MAPK14, alias *p38*) and *sirtuin 1* (SIRT1) [38,39,42], and increases apoptosis with a decline of pro-survival gene expression [38]. It has been recently shown that also human Wharton's Jelly-derived MSCs (hWJ-MSCs) treated with H_2O_2 undergo premature senescence at early culture passages: these cells show typical changes in morphology [43], slow their proliferation [44,45], result positive for SA β -Gal [43,44], express typical senescence [43] and pro-apoptotic gene markers, while displaying a down-regulation of survival genes [44,46].

The aim of the present study was to investigate and compare the effects of H_2O_2 on morphology, proliferation and senescence in hASCs and hWJ-MSCs, as representative of adult and perinatal tissues derived hMSCs, respectively. In particular, we investigated along time the effects of H_2O_2 supplied to hMSCs at different concentrations (ranging from 50 to 400 μ M), for 1 or 2 hours (h), at low and high subculture passages.

The hASCs are commonly used in cell-based therapy since their isolation is minimally invasive and because they are abundant and rapid in proliferation. On the other hand, in the human body, these cells, as well as all other adult MSCs, exhibit an age-dependent decline in their repairing capacity, increasing their susceptibility to degenerative diseases, cell death and senescence processes. In fact, multiple studies showed that the age of tissue donors affects several properties of the cells [47-49]. In particular, aged hASCs are significantly compromised in their ability to support the vascular network formation, owing to alterations in angiogenic properties [50], and their genes, normally related to senescence, act as positive regulators of apoptosis [51].

On the other hand, neonatal MSCs such as hWJ-MSCs, in their short prenatal life are not so influenced by age [52,53]. These cells express mesenchymal but not endothelial and hematopoietic markers [54,55] and display several features of embryonic stem cells (ESCs) although with a minor

expression of pluripotency genes [56-58], explaining the lack of tumorigenicity of hWJ-MSCs [59,60].

The high efficiency of hWJ-MSC recovery compared with hASCs (1 to 5×10^4 cells/cm of umbilical cord, while 1 g of adipose tissue yields approximately 5×10^3 stem cells) [61,62], the minimal ethical concerns associated with their use, their ability to modulate immunological responses and the fact that they are from young donors make them an ideal source of MSCs for therapeutic applications in allogeneic settings. Moreover, hWJ-MSCs are preferable to other stem cells isolated from perinatal tissues (*i.e.* fetal membranes) because their isolation guarantees the absence of contaminating maternal cells [52].

Therefore, the comparison between the hASC and hWJ-MSC response to oxidative stress can be useful to study the biological mechanisms at the basis of hMSC senescence and could provide two OSIPS models amenable to test putative anti-senescence modulators and develop anti-senescence strategies.

Materials and Methods

A comprehensive overview of the experimental procedures that have been used in this study was described in Figure 1.

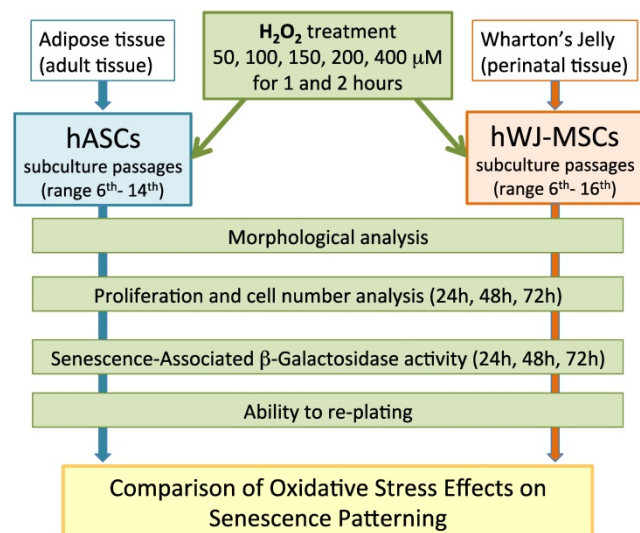


Figure 1. Comprehensive overview of the experimental procedures.

hASCs and hWJ-MSCs: harvesting and culture

All tissue samples were obtained from subjects that gave their informed consent for inclusion before they participated in the study. The study was conducted in accordance with the Declaration of Helsinki, and the protocol was approved by the local Ethical Committees (CE) (S.Orsola-Malpighi University Hospital - project identification code:

n.1645/2014, ref. 35/2014/U/Tess and Villalba Hospital - project identification code: 16076 of Bologna, Italy). hASCs have been isolated by Lipogems device (PCT/IB2011/052204) and characterized according to standard procedures and with ethical clearance, as previously described [63]. hASCs were cultured in alpha-Minimal Essential Medium (α -MEM, Carlo Erba Reagents, Milano, Italy) supplemented with 10% heat-inactivated Fetal Bovine Serum (FBS) (Gibco, Waltham, MA, USA), 1% Penicillin-Streptomycin Solution, 1% L-Glutamine 200 mM (Carlo Erba Reagents) [64]. hWJ-MSCs have been isolated from umbilical cords from healthy donor mothers and characterized as previously described [65,66]; cells were cultured in Dulbecco's Modified Eagle's Medium (DMEM) low glucose (BioWhittaker Cambrex, Walkersville, MD, USA) supplemented with 10% FBS (Gibco) and 1% Penicillin-Streptomycin Solution. Both hASCs and hWJ-MSCs were maintained at standard culture conditions of 37°C with 5% carbon dioxide in a humidified atmosphere. The non-adherent cells were removed, medium was changed twice a week and at 80% confluency cells were detached by treatment with trypsin-EDTA (Sigma-Aldrich Co., St. Louis, MO, USA), maintained and expanded until desired experimental culture passages. Both hASCs and hWJ-MSCs were derived from four healthy donors.

Hydrogen peroxide treatment

In order to test hydrogen peroxide (H_2O_2 , Sigma-Aldrich Co.) capacity to induce cell senescence, hASCs and hWJ-MSCs were treated with different H_2O_2 concentrations and then submitted to a Resazurin-based proliferation (Sigma-Aldrich Co.) or to a SA β -Gal (Sigma Aldrich Co.) assays. Cells were incubated at 37°C in complete cell culture medium containing H_2O_2 for 1 or 2 h. Untreated cells were considered as controls. In preliminary experiments, cells to be used for the cell counts and proliferation assay were exposed to five H_2O_2 concentrations (50, 100, 150, 200 or 400 μ M), while cells to be used for SA β -Gal assay, were treated with the same H_2O_2 concentrations, except for the 50 μ M. In the following experiment settings, H_2O_2 400 μ M was excluded. Moreover, a gene expression analysis was performed after 48 h from the end of the H_2O_2 stimulus: hASCs and hWJ-MSCs were treated for 2 h with H_2O_2 150 or 200 μ M respectively.

Cell count

hASCs and hWJ-MSCs, both obtained from one healthy subject (subculture passages 9th and 8th, respectively), were used in three different experiments: they were seeded in 24-well plates at the density

of 4000 and 3500 cells/cm², respectively. After 24 h in standard conditions, cells were exposed for 2 h at H₂O₂ 50, 100, 150, 200 and 400 μM or unexposed (control cells) in technical duplicate. At the end of the treatment, fresh medium was added in all the wells and culture plates were incubated in standard conditions until the count test. At 24, 48 and 72 h from the end of the *stimulus*, cells were detached by trypsin-EDTA and resuspended in a medium with 50% Eritrosyn B dye 0.2% in PBS (Sigma-Aldrich); counts were done under a light microscope at least twice with a Neubauer chamber (BRAND GmbH, Wertheim, Germany) and the cell number was calculated following the manufacturer's specifications.

Cell metabolic activity and proliferation

To evaluate the proliferation as function of metabolic activity of the cells, the "In vitro toxicology assay kit - Resazurin based" (Sigma-Aldrich Co.) was used. In this assay, metabolically active cells reduce Resazurin (not-fluorescent and blue) to Resorufin (highly fluorescent and red). Resorufin is a water-soluble compound and its intrinsic fluorescence can be measured avoiding the cell lysis (necessary with tetrazolium-salt based assays, *i.e.* MTT test). This allows to monitor cell proliferation of the same sample over time [67]. A preliminary proliferation study was conducted in order to determine the hASC and hWJ-MSC adequate cell density for seeding (data not shown). On the basis of results, hASCs and hWJ-MSCs were seeded in quadruplicates in a 96-well plate (BD Biosciences, Milano, Italy) at 4000 cells/cm² or 3500 cells/cm² respectively, in each experiment.

To determine the hASC and hWJ-MSC growth curves and to compare their basal proliferation, both hASCs and hWJ-MSCs were recovered from 4 healthy subjects (passages of subculture spanning from 6th to 14th and from 6th to 16th, respectively). Then, in order to preliminarily evaluate the toxicity of H₂O₂ treatment, both hASCs and hWJ-MSCs (9th and 8th subculture passage, respectively) were obtained from one subject and cells were treated in a technical quadruplicate with H₂O₂ at 5 different concentrations (50, 100, 150, 200 and 400 μM) for 1 and 2 h. Later, in order to evaluate the effect of selected H₂O₂ concentrations on hASC and on hWJ-MSC proliferation, experiments (in technical quadruplicate) were performed with cells obtained from 4 healthy subjects (passages of subculture spanning from 6th to 14th and from 6th to 16th, respectively). Finally, to perform a comparative analysis of cell proliferation throughout four different culture passages in hASCs (6th, 9th, 11th and 14th) and in hWJ-MSCs (6th, 8th, 11th and 16th), three different experiments were performed with cells derived from the same subject at each

studied culture passage.

In every experimental test, after 24 h from the cell seeding in standard conditions, treated cells were exposed to H₂O₂ as described above and control cells were cultured in complete medium. At the end of treatment time, fresh complete medium with Resazurin reagent (at the ratio of 10:1 respectively) was added to each well and cells were incubated at 37°C. As a negative control Resazurin solution was added to the medium without cells; we also included the totally reduced Resazurin to the medium without cells as a positive control. The fluorescence signal was measured with the Wallac 1420 Victor2 Multilabel Counter (Perkin Elmer, Waltham, MA, USA) at wavelength of 590 nm using an excitation wavelength of 560 nm. Fluorescence was measured after 2, 4, 24, 48 and 72 h from the end of the treatment. The number of viable cells correlating with the magnitude of dye reduction was expressed as percentage of Resazurin reduction according to this formula: (FI 590 of test agent - FI 590 of negative control)/(FI 590 of 100% reduced of Resazurin - FI 590 negative control) × 100 where FI is Fluorescence Intensity.

Senescence-Associated β-Galactosidase assay

To evaluate the SA β-Gal activity, the "Senescence Cells Histochemical Staining Kit" (Sigma-Aldrich Co.) was used. hASCs and hWJ-MSCs were seeded in 24-well plates (BD Biosciences) at the density of 4000 and 3400 cells/well, respectively. These specific cell densities were determined after a preliminary growth curve analysis (data not shown). After 24 h in standard conditions, cells were exposed to H₂O₂ as described above. A preliminary study was performed in triplicate for each treatment on hASCs and hWJ-MSCs derived from one subject (9th and 8th culture passage, respectively), and SA β-Gal assay was carried out after 24, 48 or 72 h from the end of the exposure to H₂O₂. Then SA β-Gal staining was investigated at 48 h using cells from three different subjects (n=3, culture passages ranging from 6th and 9th) for each cell type. The assessment of SA β-Gal activity was carried out according to the manufacturer's instructions and the positive blue staining was used as a biomarker of cellular senescence. The number of positive (blue) and negative (not colored) cells was counted in each sample in at least three random fields under a light microscope (at 200× magnification and bright field illumination) [68]. To avoid staining due to cell confluence rather than to proliferative senescence, assay was performed in sub-confluent cultures displaying comparable cell density.

Capacity of cells to undergo passages post H₂O₂ treatments

In order to test the remaining adhesion cell capacity after H₂O₂ treatment, when cultures reached 80% confluency, cells were re-seeded in 24-well plates (BD Biosciences). Control cells were splitted with 1:3 ratio, while H₂O₂-treated cells were seeded with 1:1 ratio. Cells were analyzed the following days in order to identify the proliferation cell capacity and the complete growth arrest.

Morphological analysis of senescent H₂O₂-treated cells

Cells were analyzed for morphological characteristics and changes under a light microscope (at 40× and 200× magnification) before treatment with H₂O₂, after 1 o 2 h of exposure, after 48 h from the end of the treatment and after their re-seeding. Cell images were detected under bright field illumination with the Leica MC170 HD Imaging System.

RNA extraction and RT-PCR

Cells obtained from one individual healthy subject for hASCs or hWJ-MSCs were seeded in T75 flasks at the density of 3500 cells/cm². After 24 h in standard conditions, cells were exposed to H₂O₂ 150 μM (hASCs) or 200 μM (hWJ-MSCs) for 2 h. After 48 h from the end of the *stimulus*, total RNA was extracted from treated or untreated hMSCs using the RNeasy Mini Kit (QIAGEN, Valencia, CA, USA) and digested with RNase-free Deoxyribonuclease I (DNase I) (RNase-free DNase set, QIAGEN) following the manufacturer's instructions. RNAs were reverse-transcribed as previously described [69], except for the temperature of the reaction that was 37°C instead of 42°C. The success of the reaction was verified with *glyceraldehyde 3-phosphate dehydrogenase* (*GAPDH*) gene amplification as described in [70], except for 25 cycles instead of 45; *GAPDH* amplicon detection was performed by gel agarose electrophoresis, as described by Beraudi and coll. [71]. The experiment was repeated three times.

Real time PCR

For each experimental condition, 25 ng of cDNA were amplified using the SsoAdvanced Universal SYBR Green Supermix (Bio-Rad Laboratories, Hercules, CA, USA) in technical triplicates in a Bio-Rad CFX96 real-time thermal cycler (Bio-Rad Laboratories), as previously described [70]. Specific primers for *p53* and *p21* genes were designed by Bio-Rad and used following the manufacturer's instructions (*TP53* and *CDKN1A*, 20×, Bio-Rad Laboratories). Relative gene expression was

determined by CFX Manager Software version 3.1 (Bio-Rad Laboratories) using *hypoxanthine phosphoribosyl transferase 1* (*HPRT1*), *TATA box binding protein* (*TBP*), *GAPDH* (20×, Bio-Rad Laboratories) as reference genes with the "delta-delta CT method" [72,73].

Statistical analysis

Data obtained from the *in vitro* toxicology assay were analyzed using one-way ANOVA followed by the Tukey HSD and Student's T-test. Data obtained from cell count assay were analyzed using one-way ANOVA followed by the Tukey HSD. Data obtained from real time PCR were analyzed by the CFX Manager Software version 3.1 (Bio-Rad Laboratories). Results were considered statistically significant with a p-value < 0.05 and highly significant with a p-value < 0.01.

Results

Basal cell proliferation and senescence: a comparison between human ASCs and WJ-MSCs

As previously described, the Resazurin-based assay allowed a cell proliferation monitoring over-and real-time, due to the Resorufin atoxicity [67]. On the basis of preliminary evaluations on hASC and hWJ-MSC growth curves (data not shown), cells were seeded at different concentrations (4000 cells/cm² and 3500 cells/cm², respectively) to perform proliferation experiments. In order to compare the cell metabolism of hASCs and hWJ-MSCs, results were expressed as growth rates, calculated as the percentage of Resazurin reduction at each time point divided by the percentage of reduction at the 2 h from the Resazurin inoculation. As shown in Figure 2A, the hWJ-MSC growth rate was significantly greater (at 48 h and 72 h time points, p<0.05) than the one detected for hASCs (approximately twice). Cells derived from four subjects were used in each experiment for both hASCs and hWJ-MSCs related assays (passages of subculture spanning from 6th to 14th and from 6th to 16th, respectively). Since basal metabolism was higher in hWJ-MSCs than in hASCs, in the following experiments we decided to analyze hASC and hWJ-MSC proliferation starting from 4 and 2 h from Resazurin administration, respectively. hMSC senescence in basal conditions was evaluated by SA β-Gal assay. Figure 2B shows the characteristic fibroblast-like morphology of both hASCs and hWJ-MSCs, cultured at the 9th and the 8th passage, respectively. After SA β-Gal staining, in both cell types only a small percentage of blue colored cells were appreciable (Figure 2C, black arrows).

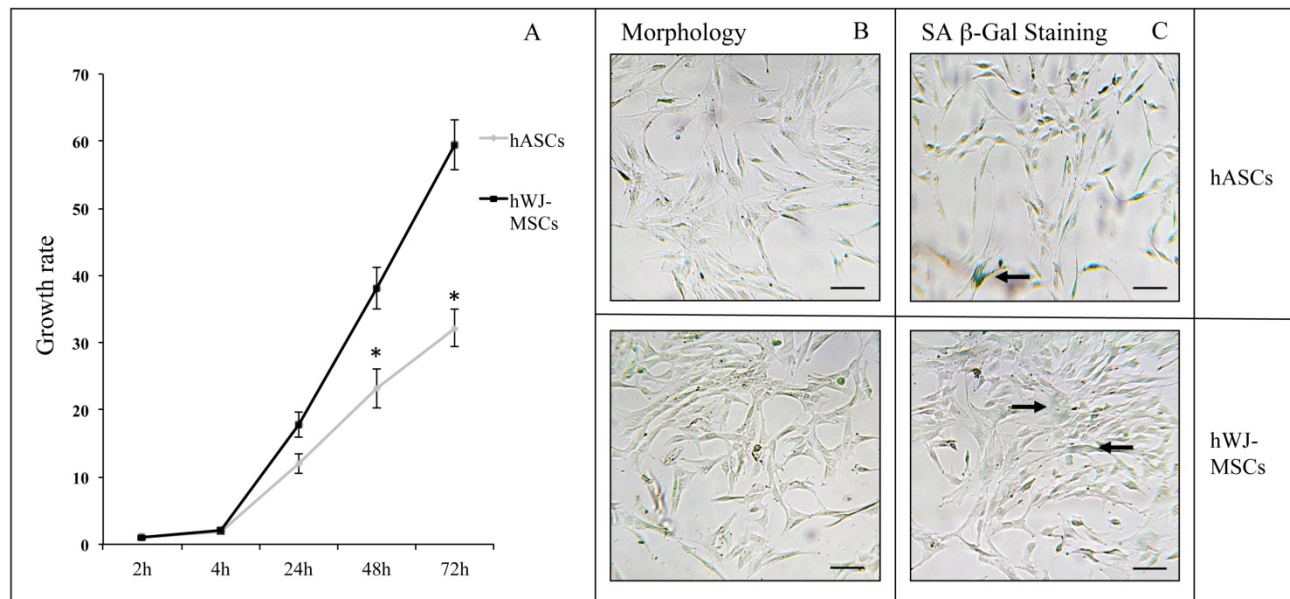


Figure 2. (A) Cell proliferation and senescence in hASCs and hWJ-MSCs: growth rate of hASCs (n=4) and hWJ-MSCs (n=4) expressed as mean \pm standard error of the mean (SEM; *p<0.05). Typical hASC and hWJ-MSC morphology at 9th- and 8th culture passages respectively (B), and SA β -Gal staining in hASCs and hWJ-MSCs (C). Cells were analyzed under a light microscope and cell images were detected under bright field illumination with the Leica MCI70 HD Imaging System at 200 \times magnification. Scale bars: 100 μ m. Representative blue cells, as markers of senescence, are indicated by black arrows.

Preliminary screening of H₂O₂ treated cells: proliferation analysis

hASCs and hWJ-MSCs cell count was performed after 24, 48 and 72 h from the end of H₂O₂ treatment (50, 100, 150, 200 and 400 μ M) for 2h. Data shown in Figure 3 (Panels A and B) were expressed as growth rates, calculated as the cell number at each time point divided by the cell number of seeded cells. Results underline that, in each experimental point, both hASCs and hWJ-MSCs treated with H₂O₂ were less in number comparing with untreated cells in a dose-dependent manner.

Moreover, a preliminary Resazurin based assay was performed to evaluate the toxicity of H₂O₂ on hASCs and hWJ-MSCs proliferation (derived from one subject at 9th and 8th subculture passage, respectively). The assay was performed after treatment with H₂O₂ at 5 different concentrations (50, 100, 150, 200 and 400 μ M) for 1 and 2 h. In Figure 3 (Panels C and D) we show the percentage of Resazurin reduction in presence or absence of a 2-h H₂O₂ treatment until 72 h post-treatment, expressed as the mean of technical quadruplicates. H₂O₂ treatment at 50, 100, 150 and 200 μ M seems to act in a dose-dependent manner on cell metabolic activity in both the hMSC types, while 400 μ M H₂O₂ induced an evident cell proliferation arrest in hASCs (Figure 3C). Similar results were obtained when H₂O₂ was administered for 1 h (data not shown).

In order to compare hASCs and hWJ-MSCs

behavior, we decided to exclude the 400 μ M higher concentration from the subsequent experimental plan.

Effect of H₂O₂ on hASC proliferation

We analyzed hASC proliferation up to 72 h following the termination of 1- or 2-h treatment in the presence of H₂O₂ at concentrations ranging from 50 to 200 μ M. Cells were obtained from four healthy subjects (passages of subculture spanning from 6th to 14th). We observed a decrease in the percentage of Resazurin reduction in H₂O₂-treated cells compared with untreated cells (Figure 4). After 1 h of H₂O₂ treatment (Figure 4, light grey lines), the differences between treated and untreated (control) cells were statistically significant (p<0.05) at 48 h when treatment was in the presence of 150 μ M H₂O₂ (Figure 4C), or at both 48 and 72 h when 200 μ M H₂O₂ was used (Figure 4D). Cell exposure to H₂O₂ for 2 h (Figure 4, dark grey lines), further enhanced the significance of experimental outcomes. In particular, while among the lower concentrations (50 and 100 μ M), 100 μ M H₂O₂ affected proliferation (p<0.05) after 24 h (Figure 4A and 4B), a 2-h treatment with higher concentrations (150 and 200 μ M) of H₂O₂ significantly decreased cell proliferation at multiple time points: after 24 (p<0.01) and 48 (p<0.05) h from the treatment with both 150 μ M and 200 μ M H₂O₂, and even after 72 h (p<0.05) in cells exposed to this latter concentration (Figure 4C and 4D).

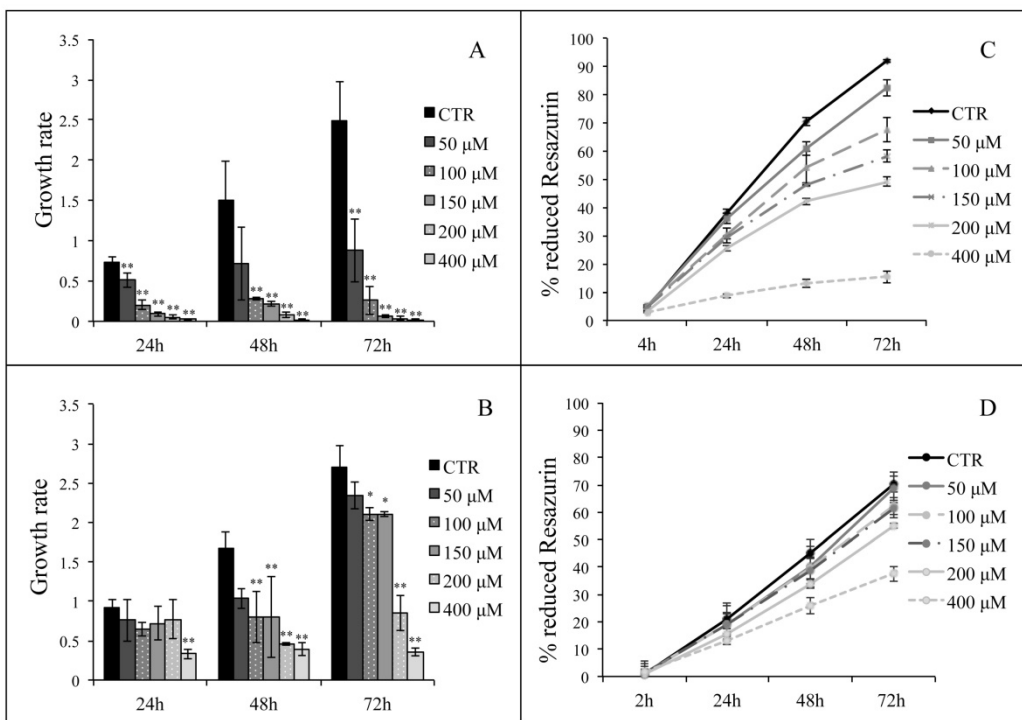


Figure 3. Panels A and B: hASCs (A) and hWJ-MSCs (B) cell counts, expressed as growth rates, calculated as the cell number at each time point divided by the cell number of seeded cells. Data are expressed as mean of growth rates \pm SD (n=3, *p<0.05, **p<0.01). Panels C and D: percentage of reduction of Resazurin (as indicator of cell proliferation) after treatment of hASCs (C) and hWJ-MSCs (D) for 2 h with H₂O₂ (50, 100, 150, 200 or 400 μ M). Analysis was conducted on a technical quadruplicate at 4, 24, 48, 72 h (C) or at 2, 24, 48, 72 h (D) from the end of the treatment and data are expressed as mean \pm SD.

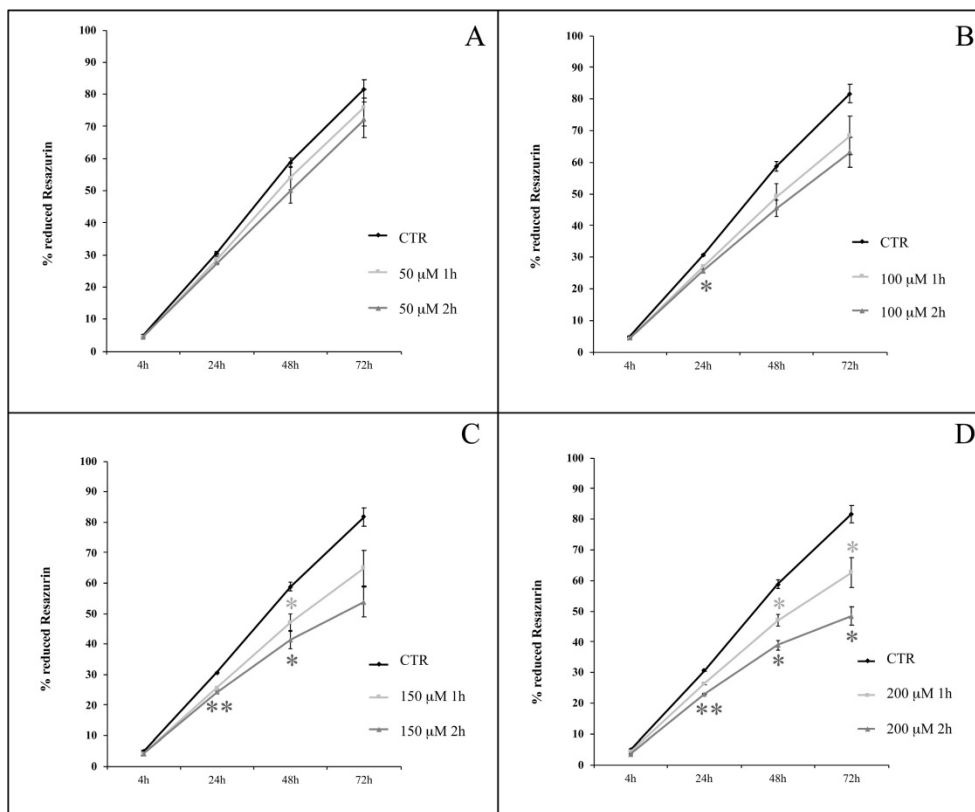


Figure 4. hASC proliferation curves after treatments with H₂O₂ at concentrations of 50 μ M (A), 100 μ M (B), 150 μ M (C) and 200 μ M (D) for 1 or 2 h. Analysis was conducted at 4, 24, 48, 72 h from the end of the treatment; data are expressed as mean of percentage of reduction of Resazurin (n=4, culture passages 6th- 14th) \pm SEM, *p<0.05, **p<0.01. CTR is control.

Since the presence of 200 μM H_2O_2 for 2-h treatment induced in hASCs the most evident reduction of cell proliferation, we also decided to perform comparative analysis of cell proliferation throughout four different culture passages (p6, p9, p11 and p14), in which these cells may intrinsically differ in senescence susceptibility, following a 2-h treatment in the presence of 200 μM H_2O_2 . As shown in Figure 5, we observed that, irrespective of the time spent in culture at different passages, H_2O_2 -exposed hASCs shared a similar proliferation decrease in comparison with the related control cells.

Effect of H_2O_2 on hWJ-MSC proliferation

In Figure 6, we show the proliferation curves of hWJ-MSCs treated for 1 and 2 h with H_2O_2 at concentrations ranging from 50 to 200 μM . Cells were obtained from four healthy subjects (passages of subculture spanning from 6th to 16th). H_2O_2 at 50, 100 and 150 μM had a weak effect on hWJ-MSCs (Figure 6A, 6B and 6C), while a 2-h exposure to the higher concentration of H_2O_2 (200 μM) resulted in a significant decrease in the percentage of Resazurin reduction, as compared with control cells. This was evident at 24, 48 and 72 h following termination of the H_2O_2 treatment ($p < 0.05$) (Figure 6D).

As for hASCs, we analyzed cell proliferation in hWJ-MSCs throughout four distinct subculture passages (p6, p8, p11 and p16): it was evident that exposed and unexposed cells exhibited a differential

response as a function of the time spent in culture (Figure 7). In fact, in early passages (*i.e.* p6) proliferation was not affected from the treatment at any time point. In contrast, in late passages (*i.e.* p11 and p16) proliferation always decreased in treated cells compared with control cells (Figure 7).

Effect of H_2O_2 on hASC SA β -Galactosidase activity

We first evaluated the H_2O_2 effect on SA β -Gal activity in hASCs (at subculture passage 9th) recovered from one healthy subject (in technical triplicate). H_2O_2 was used at the final concentrations of 100, 150, 200 and 400 μM for 1 and 2 h, and the assay was performed after 24, 48 and 72 h from the termination of the *stimuli*. At each experimental time point, 400 μM H_2O_2 produced a toxic effect and for this reason such a high concentration was not used for the assessment of SA β -Gal expression (data not shown). In all investigated conditions, H_2O_2 increased the enzyme activity in comparison with the related controls (considered as a value of 1) (Figure 8A and Figure 8B). We arbitrarily defined a ratio greater than 3 in the percentage of blue cells in treated versus control hASCs as a proof for the effectiveness of the treatment. Under these experimental conditions, after 1 h of exposure only 150 or 200 μM H_2O_2 raised SA β -Gal staining at 48 h from the termination of the treatment (Figure 7A). On the contrary, after a 2-h treatment all the H_2O_2 concentrations tested efficaciously increased SA β -Gal activity at 48 h from the end of treatment, with a more prolonged effect lasting up to 72 h when a concentration of 200 μM H_2O_2 was used (Figure 7B).

After a critical analysis of this preliminary test, we further explored SA β -Gal activity after 48 h from the end of H_2O_2 treatment in cells that had been recovered from three healthy subjects (at subculture passages 6th-9th): in Figure 8 we also show results from a representative experiment (Figure 8C) and the corresponding culture images of H_2O_2 2-h exposure (Figure 8D). We found that the percentage of blue cells after each treatment was greater than in controls (Figure 8C) and that it reached a peak after the H_2O_2 150 μM treatment.

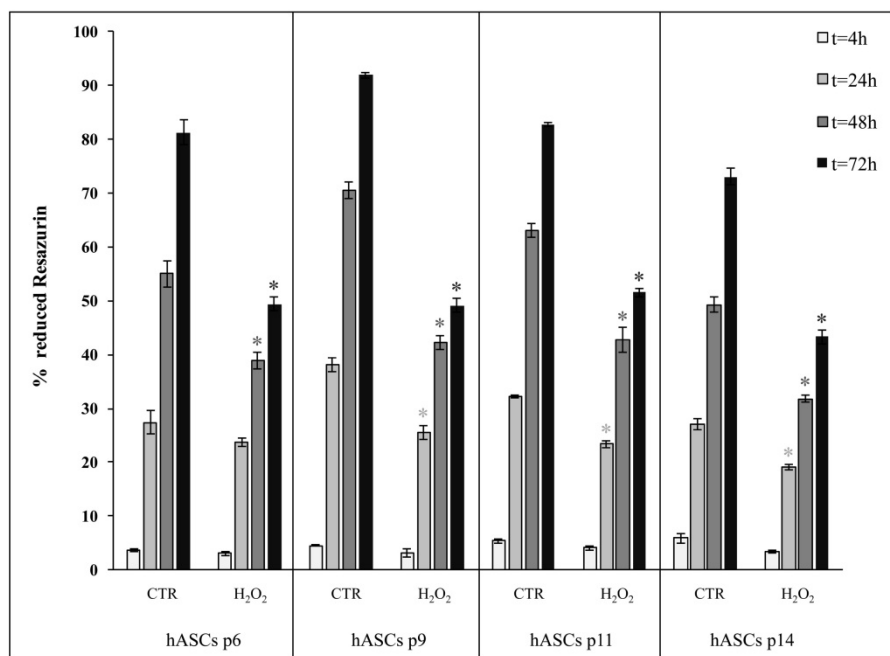


Figure 5. Comparison of cell proliferation between hASCs cultured in the absence (CTR) and presence of H_2O_2 at four subculture passages (p6, p9, p11 and p14). Treated cells were incubated with 200 μM H_2O_2 for 2 h. Data were expressed as mean of percentage of reduction of Resazurin (technical triplicate) \pm SD; * $p < 0.05$.

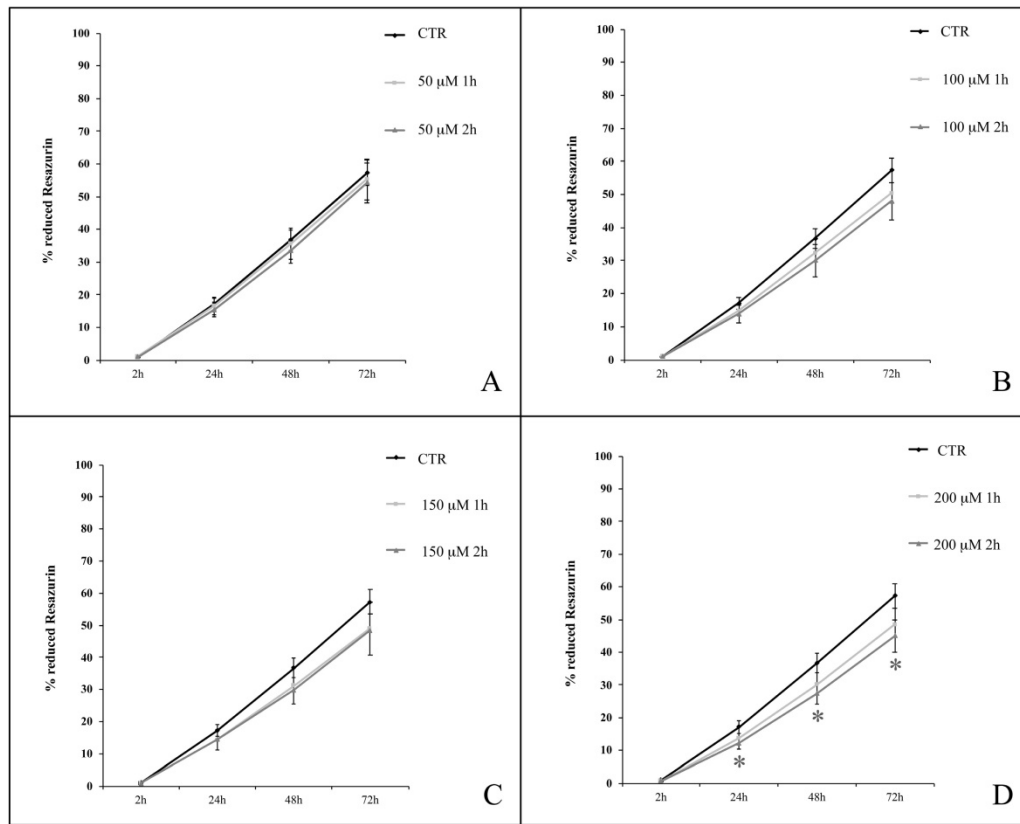


Figure 6. hWJ-MSC proliferation curves after treatment with H₂O₂ at concentrations of 50 μM (A), 100 μM (B), 150 μM (C) and 200 μM (D) for 1 or 2 h. Analysis was conducted at 2, 24, 48, 72 h from the end of the treatment; data are expressed as mean of percentage of reduction of Resazurin (n=4, culture passages 6th- 16th) ± SEM, *p<0.05. CTR is control.

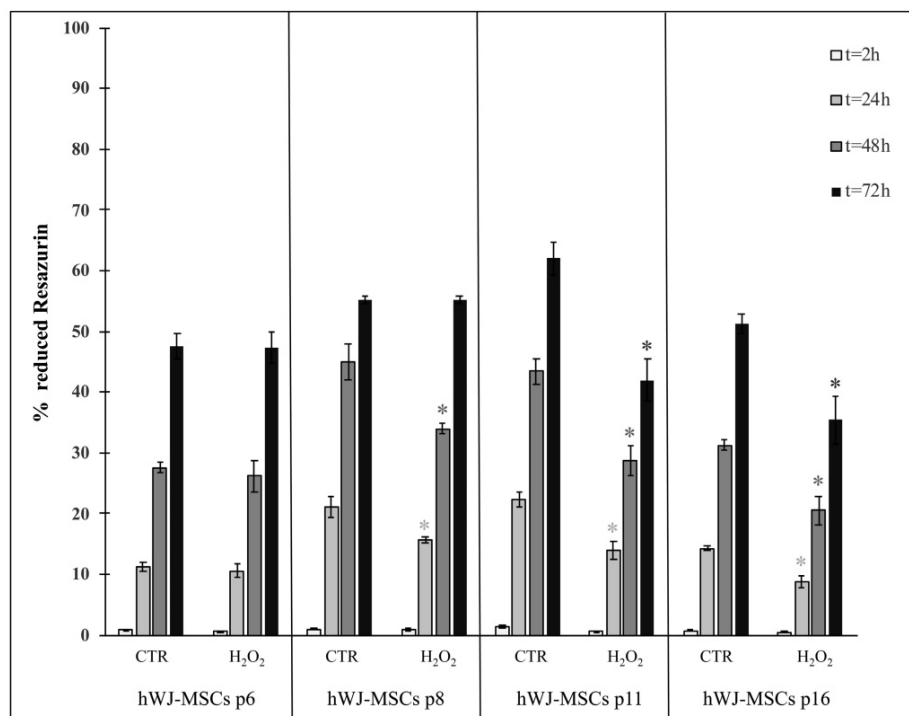


Figure 7. Comparison of cell proliferation between hWJ-MSCs cultured in the absence (CTR) and presence of H₂O₂ at four subculture passages (p6, p8, p11 and p16). Treated cells were incubated with 200 μM H₂O₂ for 2 h. Data were expressed as mean of percentage of reduction of Resazurin (technical triplicate) ± SD; *p<0.05.

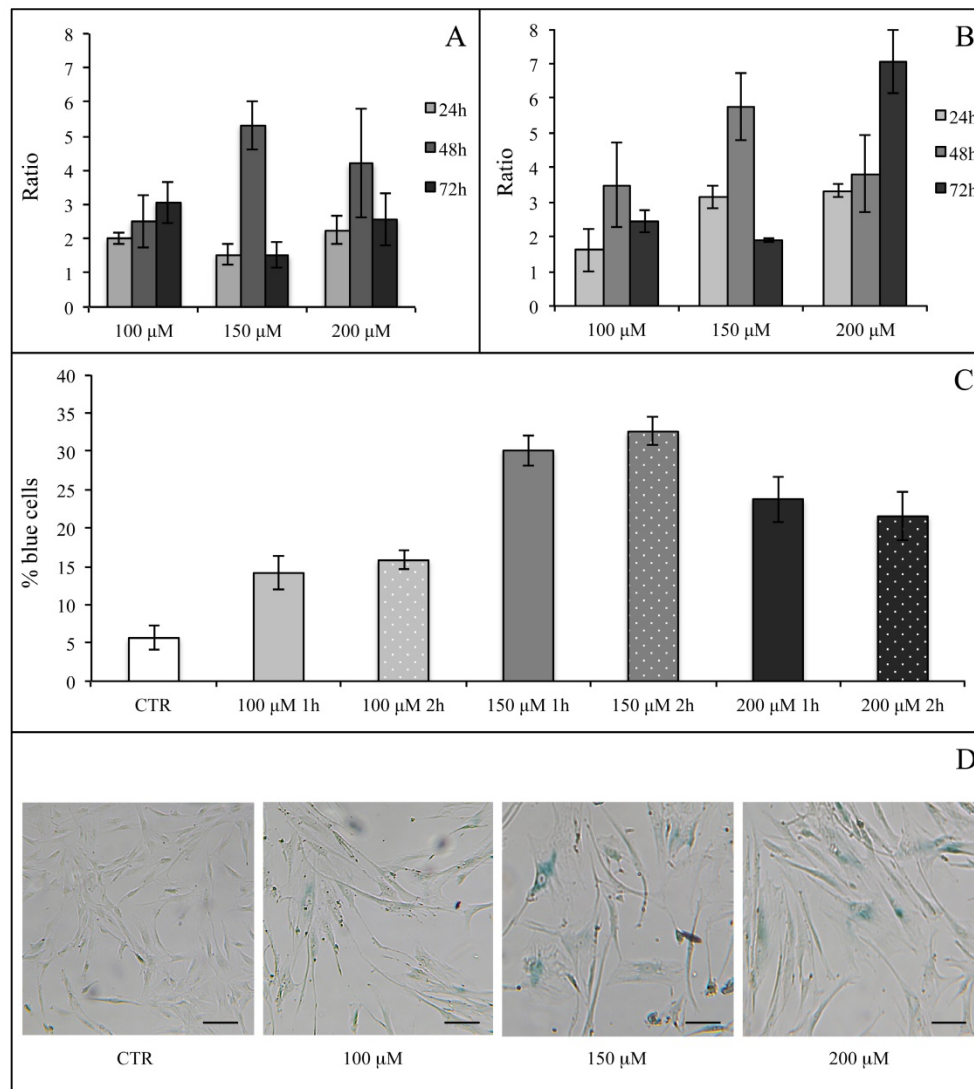


Figure 8. hASC SA β -Gal activity after H_2O_2 treatment. Effect of H_2O_2 treatment expressed in term of ratio between the percentage of blue cells in treated sample and the relative percentage of blue cells in untreated sample after 1 h (Panel A) and 2 h (Panel B) of treatment. In each panel the effect of every H_2O_2 concentration was presented after 24, 48 and 72 h from the end of the *stimulus*. Data were obtained in triplicate from one subject and expressed as ratio ($n=3$) \pm SD. Control value is 1 (not shown) and treatment was arbitrarily considered effective when ratio was >3 . In Panels (C) and (D) the effects of different H_2O_2 concentrations on hASC SA β -Gal activity tested at 48 h from the end of the treatment are shown. In Panel (C), a graph representative of three (obtained from three different subjects) showing the percentage of blue cells in untreated (CTR) and treated cells after 1 and 2 h of H_2O_2 treatment. Data were expressed as percentage of blue cells \pm SD. Panel (D): representative SA β -Gal staining images of hASCs untreated (CTR) and treated with H_2O_2 at final concentrations of 100 μ M, 150 μ M and 200 μ M after 2-h treatment. Cells were analyzed under a light microscope (at 200 \times magnification) and cell images were detected under bright field illumination with the Leica MC170 HD Imaging System. Blue staining indicates senescent cells and scale bars correspond to 100 μ m.

Effect of H_2O_2 on hWJ-MSCs SA β -Galactosidase activity

A preliminary SA β -Gal activity assay was performed in technical triplicate also on hWJ-MSCs (recovered from one healthy subject and at subculture passage 8th) after 24, 48 and 72 h from termination of the H_2O_2 treatment at concentrations of 100, 150, 200 and 400 μ M for 1 and 2 h. As seen for hASCs, cells treated with H_2O_2 400 μ M were not analyzed due to the cytotoxicity of the treatment (data not shown).

In all experimental conditions, H_2O_2 treatments (as compared with controls, corresponding to a value 1) increased the enzyme activity, and consequently

the percentage of blue stained senescent cells (Figure 9). The effectiveness of treatment was arbitrarily defined as reported in the paragraph "Effect of H_2O_2 on hASCs SA β -Galactosidase activity". We found that the most pronounced effect was detected at 48 h from the end of the treatments: after 1 h of exposure, an increase in the number of positive blue cells could only be observed in the presence of 200 μ M H_2O_2 (Figure 9A), while when cells were treated for 2 h, all H_2O_2 concentrations were effective (Figure 9B). Based upon these results, SA β -Gal activity was assessed after 48 h from the end of the H_2O_2 treatments in hWJ-MSCs harvested from three healthy subjects (at

subculture passages 6th-9th): in Figure 9, we also show results from a representative experiment (Figure 9C) and the corresponding culture images of H₂O₂ 2-h exposure (Figure 9D). H₂O₂ administration gave an increased percentage of blue cells in comparison with control hWJ-MSCs (Figure 9C). This augmentation was dependent upon both the concentration used and the duration of treatment.

Capacity of cells to undergo passages and morphological changes post H₂O₂ treatments

All investigated cell types were able to undergo culture passages post-H₂O₂ administration, revealing

differences related to H₂O₂ concentrations. In fact, while the hMSC growth was found to be slowed down after treatment with H₂O₂ 400 μ M, and the cells were not further viable on re-plating, cells that had been treated with 100, 150 and 200 μ M H₂O₂ were still able to undergo at least 2 passages. Furthermore, after increasing H₂O₂ concentration and time of exposure, hASCs and hWJ-MSCs changed their morphology at the end of the treatment, at 48 h post treatment and after the re-seeding (Figure 10 and 11). In particular, hASCs become thinner and longer (Figure 10), while hWJ-MSCs enlarged and ramified (Figure 11).

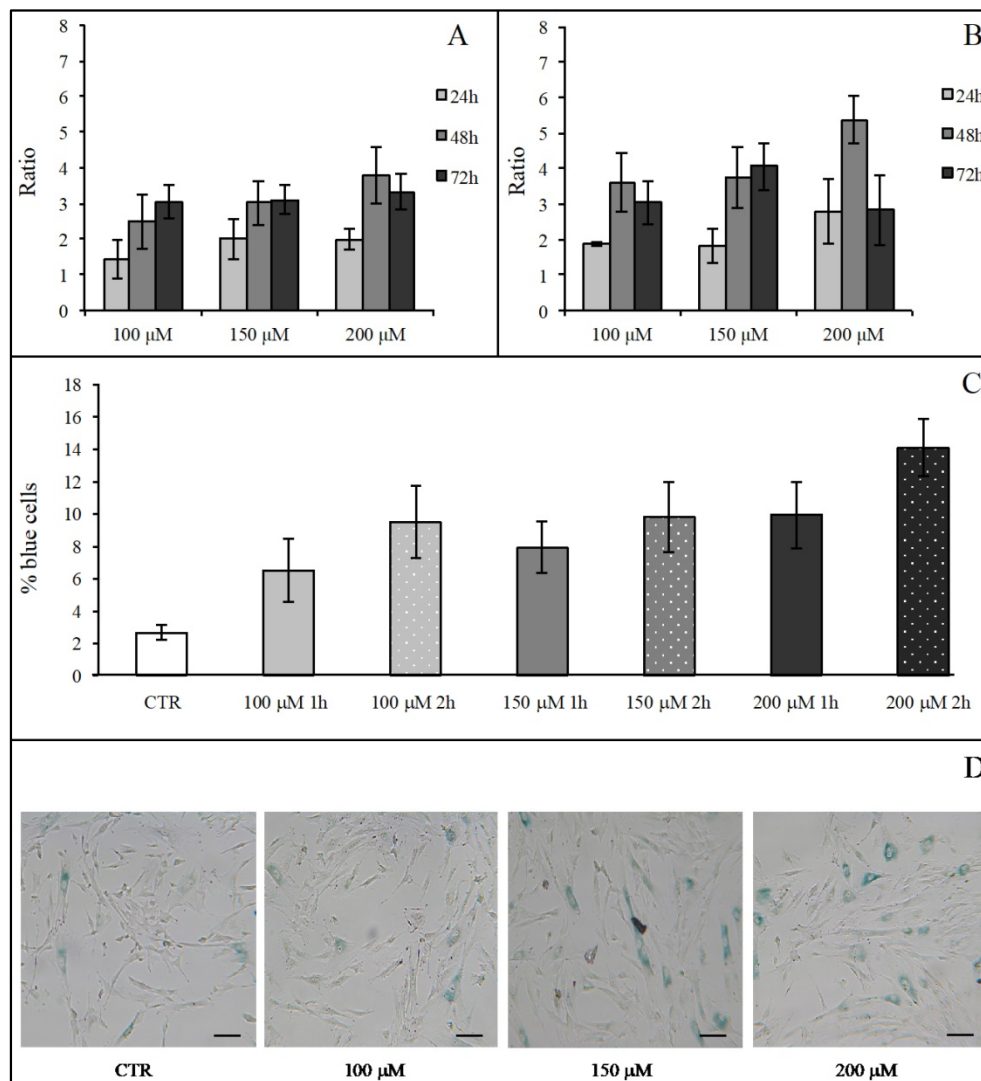


Figure 9. hWJ-MSC SA β -Gal activity after H₂O₂ treatment. Effect of H₂O₂ treatment expressed in term of ratio between the percentage of blue cells in treated sample and the relative percentage of blue cells in untreated sample after 1 h (Panel A) and 2 h (Panel B) of treatment. In each panel the effect of every H₂O₂ concentration was presented after 24, 48 and 72 h from the end of the *stimulus*. Data were obtained in triplicate from one subject and expressed as ratio ($n=3$) \pm SD. Control value is 1 (not shown) and treatment was arbitrarily considered effective when ratio was >3 . In Panels (C) and (D) the effects of different H₂O₂ concentrations on hWJ-MSC SA β -Gal activity tested at 48 h from the end of the treatment are shown. In Panel (C), a graph representative of three (obtained from three different subjects) showing the percentage of blue cells in untreated (CTR) and treated cells after 1 and 2 h of H₂O₂ treatment. Data were expressed as percentage of blue cells \pm SD. Panel (D): representative SA β -Gal staining images of hWJ-MSCs untreated (CTR) and treated with H₂O₂ at final concentrations of 100 μ M, 150 μ M and 200 μ M after 2-h treatment. Cells were analyzed under a light microscope (at 200 \times magnification) and cell images were detected under bright field illumination with the Leica MC170 HD Imaging System. Blue staining indicates senescent cells and scale bars correspond to 100 μ m.

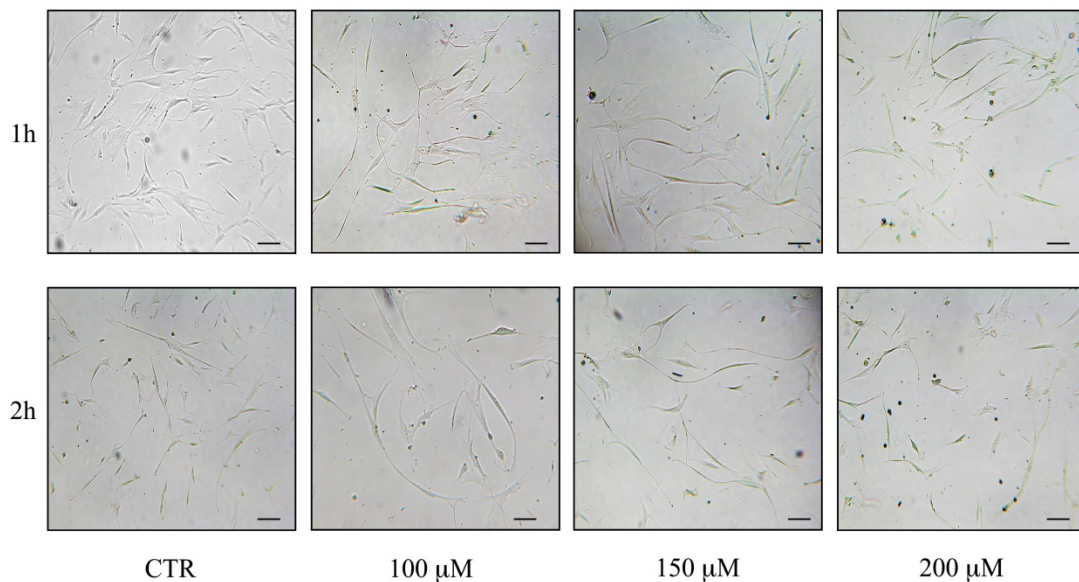


Figure 10. Morphological changes of hASCs after reseeding post H_2O_2 treatments: control (CTR) cells and cells treated with H_2O_2 100, 150 and 200 μM . Cells were analyzed under a light microscope (at 200 \times magnification) and cell images were detected under bright field illumination with the Leica MC170 HD Imaging System. Scale bars: 100 μm .

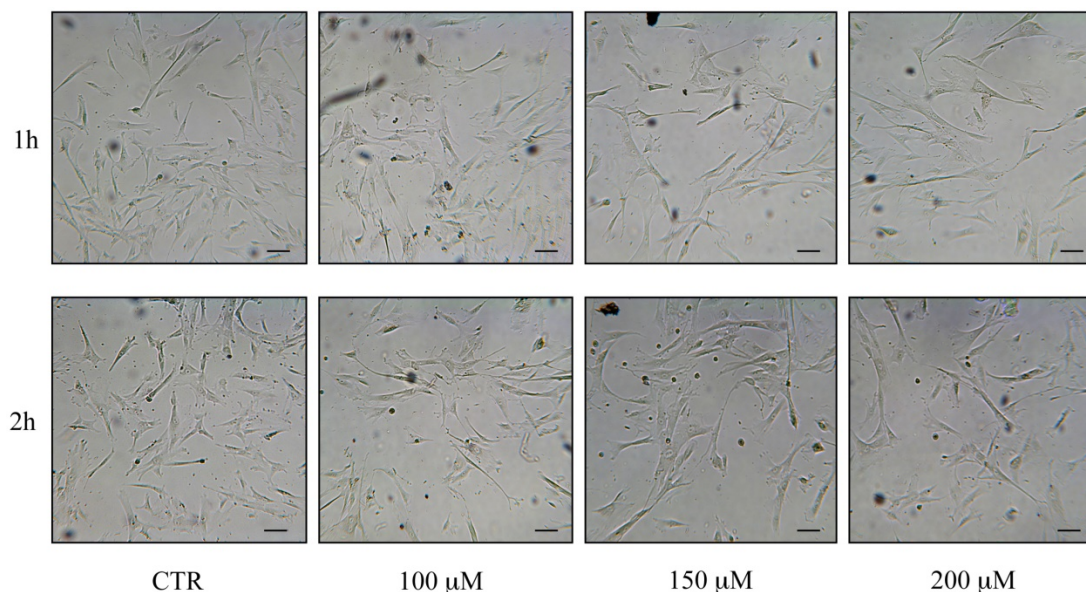


Figure 11. Morphological changes of hWJ-MSCs after reseeding post H_2O_2 treatments: control (CTR) cells and cells treated with H_2O_2 100, 150 and 200 μM . Cells were analyzed under a light microscope (at 200 \times magnification) and cell images were detected under bright field illumination with the Leica MC170 HD Imaging System. Scale bars: 100 μm .

Effect of H_2O_2 on hMSCs gene expression

p21 and *p53* expression was investigated at 48 h from the end of the H_2O_2 specific treatment both in hASCs (*i.e.* 150 μM for 2 h) and hWJ-MSCs (*i.e.* 200 μM for 2 h). As depicted in Figure 12, hydrogen peroxide strongly acted on *p21* overexpression in hMSCs independently of their source ($p < 0.01$). At the same time, H_2O_2 treatment in hASCs resulted in a down regulation of *p53* (Figure 12A), while in hWJ-MSCs it shows a stable expression in comparison with the control (Figure 12B).

Discussion

Both hASCs and hWJ-MSCs are frequently used in stem cell-based protocols [2]. These cells undergo significant decline in their rescuing potential as they age *in vivo* during the lifespan, or when they become senescent during their expansion *in vitro*, with significant impairment in the outcome of cell therapy efforts [22-24].

The availability of reliable accelerated methods to induce stem cell senescence *in vitro* will avoid

cumbersome long-lasting (2-3 months) culture protocols and facilitate the investigation of senescence mechanisms and source-related senescence susceptibility among different hMSC populations [13].

To this end, we observed that hASCs and hWJ-MSCs exhibited different proliferation profiles over time, indicating that basal metabolism may be higher in hWJ-MSCs than in hASCs. Akin to this observation is the present finding that hWJ-MSCs required a greater number of culture passages than hASCs for undergoing senescence, as it can also be inferred from the ability of hWJ-MSCs to exhibit long-lasting stemness properties and preserve a typical fibroblast-like morphology while undergoing multiple culture passages *in vitro* [43,74].

Here, we found that in both cell populations, H₂O₂ not only inhibited cell proliferation in a dose-dependent fashion, but it also affected the persistence of the anti-proliferative effect after the end of exposure (up to 48 or 72 h) in a manner that was dependent upon the duration (1 or 2 h) of the treatment itself. These results are coherent with the reduction of cell vitality observed in hWJ-MSCs [43-45] and hASCs [39,42] treated with higher concentrations of H₂O₂ (until 2000 μ M) but at low subcultured passages. We also observed a growth slowdown of cells treated with H₂O₂ 400 μ M, and a cell inability to re-plate. On the other hand, cells treated with 100, 150 and 200 μ M H₂O₂ were still able to undergo at least 2 passages, although an increase in H₂O₂ concentration and exposure time were associated to morphology changes. These results were consistent with those obtained in the study of Choo and coll. (2014), where hWJ-MSCs exposed to H₂O₂ resulted enlarged, with cytoplasm enriched of granules and able to undergo until 3-4 passages after H₂O₂ treatment [43].

The possibility that the observed difference in

basal proliferative activity among hASCs and hWJ-MSCs may entail different senescence susceptibilities [13,75] was confirmed by the finding that the same H₂O₂ concentrations that remarkably inhibited proliferation in hASCs, only weakly affected hWJ-MSC proliferation, and that a significant decrease in the percentage of reduced Resazurin could be achieved in these cells solely after the exposure to the H₂O₂ concentration that proved the most effective one in hASCs. Our results are reinforced by the previous evidence that low H₂O₂ concentrations (50 and 100 μ M) did not affect hWJ-MSCs proliferation treated for 24 h [45].

The analysis of the effect of H₂O₂ treatment on proliferation in cells that had been subjected to different, even long-term subculture passages (until 14-16th), provided the chance of further compounding the multifaceted ways different hMSC populations may progress in senescence. For the first time we demonstrated that H₂O₂ given for 2 h, reduced hASC proliferation both in early and late subculture passages, while it decreased hWJ-MSC proliferation in a passage-dependent fashion, in particular only at higher subculture passages.

These observations were all corroborated by results obtained from our analysis of SA β -Gal activity after 24, 48 and 72 h from the end of the H₂O₂ treatment, where both hASCs and hWJ-MSCs showed an increase of the SA β -Gal activity. In particular, the higher senescent effect was evident at 48 h. A similar trend was seen in other researches, although it was obtained at different experimental times [42-44].

Comparing SA β -Gal assay results, it is evident that hWJ-MSCs and hASCs have a different way to respond to oxidative stress. To this end, the SA β -Gal activity increase observed in hWJ-MSCs was dependent on both H₂O₂ concentration and exposure time, reaching a maximum with 200 μ M H₂O₂ for 2 h, while hASCs showed the greatest increase with 150 μ M H₂O₂. In fact, if hASCs were exposed to H₂O₂ at low concentrations (*i.e.* 100 μ M) they were able to counteract pro-senescence stress, while if cells were treated with 200 μ M H₂O₂ they showed a SA β -Gal activity increase, although weaker than that induced by 150 μ M H₂O₂. This observation could be explained by the well documented ability of H₂O₂ to promote not only senescence but also apoptosis depending upon the experimental conditions [43,76].

The persistence of the hydrogen peroxide effects on cell senescence was shown also by the gene expression

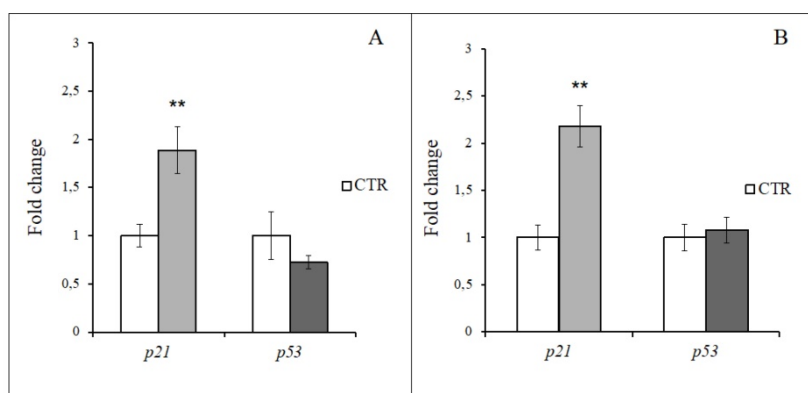


Figure 12. Gene expression analysis in hASCs and hWJ-MSCs after 48 h from 2h-H₂O₂ treatment. A: p21 and p53 relative expression in hASCs treated with 150 μ M H₂O₂. B: p21 and p53 relative expression in hWJ-MSCs treated with 200 μ M H₂O₂. Data were expressed as mean fold change (n=3) \pm SD, **p<0.01.

analysis of two of the major cell cycle regulators, *p21* and *p53*. At 48 h from the end of the most effective and specific H₂O₂ treatment, in both hMSC types the inhibition of cell cycle progression was associated with a strong overexpression of *p21*, a transient growth arrest mediator, able to slowdown cell proliferation [22]. At the same time, *p53* transcription was quite stable in hWJ-MSCs, while being down-regulated in hASCs, suggesting that after 2 days from the selected H₂O₂ administration, hMSCs did not start an apoptotic program.

Overall the present data not only provide evidence for the effectiveness of the H₂O₂ exposure method in recapitulating over time senescence features in hMSCs, but also indicate its usefulness in detecting the proneness of different hMSC populations to undergo senescence on the basis of their tissue source [13,73].

In particular, hWJ-MSCs present several advantages comparing with hASCs: not only their easy availability and isolation, their independence from donor age, but also their natural proneness to undergo senescence at late culture passages and their ability to efficiently counteract oxidative stress *stimuli*.

Moreover, within cell therapy contexts, the present study may also set the basis to investigate and establish the limit(s) for *in vitro* expansion of targeted hMSC populations in order to achieve an optimal balance between the cell number available for transplantation and the risk for cell expansion-related senescence. These considerations may also apply to the development of patient-specific protocols for the expansion of defined hMSC populations in the future perspective of Precision Medicine approaches.

Abbreviations

hASCs: human Adipose tissue-derived Stem Cells; hWJ-MSCs: human Wharton's Jelly-derived Mesenchymal Stem Cells; H₂O₂: hydrogen peroxide; hMSCs: human Mesenchymal Stem Cells; SA β-Gal: Senescence-Associated β-Galactosidase; ROS: Reactive Species of Oxygen; OSIPS: Oxidative Stress-Induced Premature Senescence; SOD: Superoxide Dismutase; GSH: Glutathione Synthetase; MAPK14: *mitogen-activated protein kinase 14* (alias *p38*); SIRT1: *sirtuin 1*; α-MEM: alfa-Minimal Essential Medium; DMEM: Dulbecco's Modified Eagle's Medium; FBS: Fetal Bovine Serum; HPRT1: *hypoxanthine phosphoribosyl transferase 1*; TBP: TATA box binding protein; GAPDH: *glyceraldehyde 3-phosphate dehydrogenase*; CDKN1A: *cyclin dependent kinase inhibitor 1A* (alias *p21*); TP53: *tumor protein p53* (alias *p53*); p: passage; h: hour; SD: standard deviation; SEM: standard error of the mean.

Acknowledgments

This study was funded by Eldor Lab, via Vittor Pisani 16, 20124 Milan, Italy.

Competing Interests

The authors have declared that no competing interest exists.

References

- Chen C, Fingerhut JM, Yamashita YM. The ins(ide) and outs(ide) of asymmetric stem cell division. *Curr Opin Cell Biol.* 2016; 43:1-6.
- Dominici M, Le Blanc K, Mueller J, Slaper-Cortenbach I, Marini F, Krause D, Deans R, Keating A, Prockop DJ, Horwitz E. Minimal criteria for defining multipotent mesenchymal stromal cells. The International Society for Cellular Therapy position statement. *Cytotherapy.* 2006; 8(4):315-317.
- Smiler D, Soltan M, Albitar M. Toward the identification of mesenchymal stem cells in bone marrow and peripheral blood for bone regeneration. *Implant Dent.* 2008; 17(3):236-247.
- Aust L, Devlin B, Foster SJ, Halvorsen YD, Hicok K, du Laney T, Sen A, Willingmyre GD, Gimble JM. Yield of human adipose-derived adult stem cells from liposuction aspirates. *Cytotherapy.* 2004; 6(1):7-14.
- In't Anker PS, Scherjon SA, Kleijburg-van der Keur C, de Groot-Swings GM, Claas FH, Fibbe WE, Kanhai HH. Isolation of mesenchymal stem cells of fetal or maternal origin from human placenta. *Stem Cells.* 2004; 22(7):1338-1345.
- Corrao S, La Rocca G, Lo Iacono M, Corsello T, Farina F, Anzalone R. Umbilical cord revisited: From Wharton's jelly myofibroblasts to mesenchymal stem cells. *Histol Histopathol.* 2013; 28(10):1235-1244.
- Erices A, Conget P, Minguell JJ. Mesenchymal progenitor cells in human umbilical cord blood. *Br J Haematol.* 2000; 109(1):235-242.
- Kwon A, Kim Y, Kim M, Kim J, Choi H, Jekarl DW, Lee S, Kim JM, Shin JC, Park IY. Tissue-specific differentiation potency of mesenchymal stromal cells from perinatal tissues. *Sci Rep.* 2016; 6:23544.
- Chen JY, Mou XZ, Du XC, Xiang C. Comparative analysis of biological characteristics of adult mesenchymal stem cells with different tissue origins. *Asian Pac J Trop Med.* 2015; 8(9):739-746.
- Billing AM, Ben Hamidane H, Dib SS, Cotton RJ, Bhagwat AM, Kumar P, Hayat S, Yousri NA, Goswami N, Suhre K, Rafii A, Graumann J. Comprehensive transcriptomic and proteomic characterization of human mesenchymal stem cells reveals source specific cellular markers. *Sci Rep.* 2016; 6:21507.
- Dabrowski FA. Comparison of the paracrine activity of mesenchymal stem cells derived from human umbilical cord, amniotic membrane and adipose tissue. *J Obstet Gynaecol Res.* 2017; 43(11):1758-1768.
- Maleki M, Ghanbarvand F, Reza Behvarz M, Ejtemaei M, Ghadirkhomi E. Comparison of mesenchymal stem cell markers in multiple human adult stem cells. *Int J Stem Cells.* 2014; 7(2):118-126.
- Samsonraj RM, Raghunath M, Nurcombe V, Hui JH, van Wijnen AJ, Cool SM. Concise Review: Multifaceted Characterization of Human Mesenchymal Stem Cells for Use in Regenerative Medicine. *Stem Cells Transl Med.* 2017; 6(12):2173-2185.
- Patel DM, Shah J, Srivastava AS. Therapeutic potential of mesenchymal stem cells in regenerative medicine. *Stem Cells Int.* 2013; 2013:496218.
- Wei X, Yang X, Han ZP, Qu FF, Shao L, Shi YF. Mesenchymal stem cells: A new trend for cell therapy. *Acta Pharmacol Sin.* 2013; 34(6):747-754.
- Mahla RS. Stem cells applications in regenerative medicine and disease therapeutics. *Int J Cell Biol.* 2016; 2016:6940283.
- Bai L, Lennon DP, Caplan AI, DeChant A, Hecker J, Kranso J, Zaremba A, Miller RH. Hepatocyte growth factor mediates mesenchymal stem cell-induced recovery in multiple sclerosis models. *Nat Neurosci.* 2012; 15(6):862-870.
- Chang C, Wang X, Niu D, Zhang Z, Zhao H, Gong F. Mesenchymal stem cells adopt beta-cell fate upon diabetic pancreatic microenvironment. *Pancreas.* 2009; 38(3):275-281.
- Kuo YR, Goto S, Shih HS, Wang FS, Lin CC, Wang CT, Huang EY, Chen CL, Wei FC, Zheng XX, Lee WP. Mesenchymal stem cells prolong composite tissue allotransplant survival in a swine model. *Transplantation.* 2009; 87(12):1769-1777.
- Souza BS, Nogueira RC, de Oliveira SA, de Freitas LA, Lyra LG, Ribeiro dos Santos R, Lyra AC, Soares MB. Current status of stem cell therapy for liver diseases. *Cell Transplant.* 2009; 18(12):1261-1279.
- Quevedo HC, Hatzistergos KE, Oskoue BN, Feigenbaum GS, Rodriguez JE, Valdes D, Pattany PM, Zambrano JP, Hu Q, McNiece I, Heldman AW, Hare JM. Allogeneic mesenchymal stem cells restore cardiac function in chronic ischemic cardiomyopathy via trilineage differentiating capacity. *Proc Natl Acad Sci USA.* 2009; 106(33):14022-14027.
- Turinetto V, Vitale E, Giachino C. Senescence in Human Mesenchymal Stem Cells: Functional Changes and Implications in Stem Cell-Based Therapy. *Int J Mol Sci.* 2016; 17(7):E1164.

23. Ho AD, Wagner W, Mahlknecht U. Stem cells and ageing. The potential of stem cells to overcome age-related deteriorations of the body in regenerative medicine. *EMBO Rep.* 2005; 6:535-538.
24. Wagner W, Bork S, Horn P, Kronic D, Walenda T, Diehlmann A, Benes V, Blake J, Huber FX, Eckstein V, Boukamp P, Ho AD. Aging and replicative senescence have related effects on human stem and progenitor cells. *PLoS ONE.* 2009; 4(6):e5846.
25. Hayflick L. The limited in vitro lifetime of human diploid cell strains. *Exp Cell Res.* 1965; 37:614-636.
26. Benameur L, Charif N, Li Y, Stoltz JF, de Isla N. Toward an understanding of mechanism of aging induced oxidative stress in human mesenchymal stem cells. *Biomed Mater Eng.* 2015; 25(1 Suppl):41-46.
27. Reuter S, Gupta SC, Chaturvedi MM, Aggarwa BB. Oxidative stress, inflammation, and cancer: How are they linked? *Free Radic Biol Med.* 2010; 49(11):1603-1616.
28. Haines DD, Juhasz B, Tosaki A. Management of multicellular oxidative and oxidative stress. *J Cell Mol Med.* 2013; 17(8):936-957.
29. Chen JH, Stoeber K, Kingsbury S, Ozanne SE, Williams GH, Hales CN. Loss of proliferative capacity and induction of senescence in oxidatively stressed human fibroblasts. *J Biol Chem.* 2004; 279(47):49439-49446.
30. Passos JF, von Zglinicki T. Oxygen free radicals in cell senescence: are they signal transducers? *Free Radic Res.* 2006; 40(12):1277-1283.
31. Harmand D. Aging: a theory based on free radical and radiation chemistry. *J Gerontol.* 1956; 11(3):298-300.
32. Valle-Prieto A, Conget PA. Human mesenchymal stem cells efficiently manage oxidative stress. *Stem Cells Dev.* 2010; 19(12):1885-1893.
33. Denu RA, Hematti P. Effects of Oxidative Stress on Mesenchymal Stem Cell Biology. *Oxid Med Cell Longev.* 2016; 2016:2989076.
34. Brandl A, Meyer M, Bechmann V, Nerlich M, Angele P. Oxidative stress induces senescence in human mesenchymal stem cells. *Exp Cell Res.* 2011; 317(11):1541-1547.
35. Kim JS, Kim EJ, Kim HJ, Yang JY, Hwang GS, Kim CW. Proteomic and metabolomic analysis of H₂O₂-induced premature senescent human mesenchymal stem cells. *Exp Gerontol.* 2011; 46(6):500-510.
36. Park SY, Jeong AJ, Kim GY, Jo A, Lee JE, Leem SH, Yoon JH, Ye SK, Chung JW. Lactoferrin Protects Human Mesenchymal Stem Cells from Oxidative Stress-Induced Senescence and Apoptosis. *J Microbiol Biotechnol.* 2017; 27(10):1877-1884.
37. Zhou L, Chen X, Liu T, Gong Y, Chen S, Pan G, Cui W, Luo ZP, Pei M, Yang H, He F. Melatonin reverses H₂O₂-induced premature senescence in mesenchymal stem cells via the SIRT1-dependent pathway. *J Pineal Res.* 2015; 59(2):190-205.
38. Lee JH, Jung HK, Han YS, Yoon YM, Yun CW, Sun HY, Cho HW, Lee SH. Antioxidant effects of Cirsium setidens extract on oxidative stress in human mesenchymal stem cells. *Mol Med Res.* 2016; 14(4):3777-3784.
39. Wang N, Wang F, Gao Y, Yin P, Pan C, Liu W, Zhou Z, Wang J. Curcumin protects human adipose-derived mesenchymal stem cells against oxidative stress-induced inhibition of osteogenesis. *J Pharmacol Sci.* 2016; 132(3):192-200.
40. Baldari S, Di Rocco G, Trivisonno A, Samengo D, Pani G, Toietta G. Promotion of survival and engraftment of transplanted adipose tissue-derived stromal and vascular cells by overexpression of manganese superoxide dismutase. *Int J Mol Sci.* 2016; 17(7):1082.
41. Altanerova V, Horvathova E, Matuskova M, Kucerova L, Altaner C. Genotoxic damage of human adipose-tissue derived mesenchymal stem cells triggers their terminal differentiation. *Neoplasma.* 2009; 56(6):542-547.
42. Rajamani K, Lin YC, Wen TC, Hsieh J, Subeq YM, Liu JW, Lin PC, Harn HJ, Lin SZ, Chiou TW. The antisenesence effect of trans-cinnamaldehyde on adipose-derived stem cells. *Cell Transplant.* 2015; 24(3):493-507.
43. Choo KB, Tai L, Hymavathees KS, Wong CY, Nguyen PN, Huang CJ, Cheong SK, Kamarul T. Oxidative stress-induced premature senescence in Wharton's jelly-derived mesenchymal stem cells. *Int J Med Sci.* 2014; 11(11):1201-1207.
44. Wajid N, Mehmood A, Bhatti FU, Khan SN, Riazuddin S. Lovastatin protects chondrocytes derived from Wharton's jelly of human cord against hydrogen-peroxide-induced in vitro injury. *Cell Tissue Res.* 2013; 351(3):433-443.
45. Nimsanor N, Phetfong J, Plabplueng C, Jangpatrapongsa K, Prachayasittikul V, Supokawej A. Inhibitory effect of oxidative damage on cardiomyocyte differentiation from Wharton's jelly-derived mesenchymal stem cells. *Exp Ther Med.* 2017; 14(6):5329-5338.
46. Nouri F, Salehinejad P, Nematollahi-Mahani SN, Kamarul T, Zarrindast MR, Sharifi AM. Deferoxamine Preconditioning of Neural-Like Cells Derived from Human Wharton's Jelly Mesenchymal Stem Cells as a Strategy to Promote Their Tolerance and Therapeutic Potential: An In Vitro Study. *Cell Mol Neurobiol.* 2016; 36(5):689-700.
47. Stolzing A, Jones E, McGonagle D, Scutt A. Age-related changes in human bone marrow-derived mesenchymal stem cells: consequences for cell therapies. *Mech Ageing Dev.* 2008; 129(3):163-173.
48. Huang K, Zhou DH, Huang SL, Liang SH. Age related biological characteristics of human bone marrow mesenchymal stem cells from different age donors. *Zhongguo Shi Yan Xue Ye Xue Za Zhi.* 2005; 13(6):1049-1053.
49. Stenderup K, Justesen J, Clausen C, Kassem M. Aging is associated with decreased maximal life span and accelerated senescence of bone marrow stromal cells. *Bone.* 2003; 33(6):919-926.
50. Madonna R, Renna FV, Cellini C, Cotellese R, Picardi N, Francomano F, Innocenti P, De Caterina R. Age-dependent impairment of number and angiogenic potential of adipose tissue-derived progenitor cells. *Eur J Clin Invest.* 2011; 41(2):126-133.
51. Alt EU, Senst C, Murthy SN, Slakey DP, Dupin CL, Chaffin AE, Kadowitz PJ, Izadpanah R. Aging alters tissue resident mesenchymal stem cell properties. *Stem Cell Res.* 2012; 8(2):215-225.
52. Davies JE, Walker JT, Keating A. Concise review: Wharton's Jelly: The rich, but enigmatic, source of mesenchymal stromal cells. *Stem Cells Transl Med.* 2017; 6(7):1620-1630.
53. Kalaszczynska I, Ferdyn K. Wharton's jelly derived mesenchymal stem cells: future of regenerative medicine? Recent findings and clinical significance. *Biomed Res Int.* 2015; 2015:430847.
54. Conconi MT, Liddo RD, Tommasini M, Calore CC, Parnigotto PP. Phenotype and differentiation potential of stromal populations obtained from various zones of human umbilical cord: an overview. *Open Tissue Eng Regen Med J.* 2011; 4:6-20.
55. Anzalone R, Iacono ML, Corrao S, Magno F, Loria T, Cappello F, Zumbo G, Farina F, La Rocca G. New emerging potentials for human Wharton's jelly mesenchymal stem cells: immunological features and hepatocyte-like differentiative capacity. *Stem Cells Dev.* 2010; 19(4):423-438.
56. Nekanti U, Mohanty L, Venugopal P, Balasubramanian S, Totey S, Ta M. Optimization and scale-up of Wharton's jelly derived mesenchymal stem cells for clinical applications. *Stem Cell Res.* 2010; 5(3):244-254.
57. Tong CK, Vellasamy S, Tan BC, Abdullah M, Vidyadaran S, Seow HF, Ramasamy R. Generation of mesenchymal stem cell from human umbilical cord tissue using a combination enzymatic and mechanical disassociation method. *Cell Biol Int.* 2011; 35(3):221-226.
58. Fong CY, Chak LL, Biswas A, Tan JH, Gauthaman K, Chan WK, Bongso A. Human Wharton's jelly stem cells have unique transcriptome profiles compared to human embryonic stem cells and other mesenchymal stem cells. *Stem Cell Rev.* 2011; 7(1):1-16.
59. Rachakarla RS, Marini F, Weiss ML, Tamura M, Troyer D. Development of human umbilical cord matrix stem cell-based gene therapy for experimental lung tumors. *Cancer Gene Ther.* 2007; 14(10):828-835.
60. Kim DW, Staples M, Shinozuka K, Pantcheva P, Kang SD, Borlongan CV. Wharton's jelly-derived mesenchymal stem cells: phenotypic characterization and optimizing their therapeutic potential for clinical applications. *Int J Mol Sci.* 2013; 14(6):11692-11712.
61. Fraser JK, Wulur I, Alfonso Z, Hedrick MH. Fat tissue: an underappreciated source of stem cells for biotechnology. *Trends Biotechnol.* 2006; 24(4):150-154.
62. Weiss ML, Medcetty S, Bledsoe AR, Rachakarla RS, Choi M, Merchav S, Luo Y, Rao MS, Velagaleti G, Troyer D. Human umbilical cord matrix stem cells: preliminary characterization and effect of transplantation in a rodent model of Parkinson's disease. *Stem Cells.* 2006; 24(3):781-792.
63. Bianchi F, Maioli M, Leonardi E, Olivi E, Pasquini G, Valente S, Mendez AJ, Ricordi C, Raffaini M, Tremolada C, Ventura C. A new nonenzymatic method and device to obtain a fat tissue derivative highly enriched in pericyte-like elements by mild mechanical forces from human lipoaspirates. *Cell Transplant.* 2013; 22(11):2063-2077.
64. Canaider S, Maioli M, Facchin F, Bianconi E, Santaniello S, Pigliaru G, Ljungberg L, Burigana F, Bianchi F, Olivi E, Tremolada C, Biava PM, Ventura C. Human stem cell exposure to developmental stage zebrafish extracts: a novel strategy for tuning stemness and senescence patterning. *CellR4.* 2014; 2:e1226.
65. Paradisi M, Alviano F, Pironi S, Lanzoni G, Fernandez M, Lizzo G, Giardino L, Giuliani A, Costa R, Marchionni C, Bonsi L, Calzà L. Human mesenchymal stem cells produce bioactive neurotrophic factors: source, individual variability and differentiation issues. *Int J Immunopathol Pharmacol.* 2014; 27(3):391-402.
66. La Rocca G, Anzalone R, Corrao S, Magno F, Loria T, Lo Iacono M, Di Stefano A, Giannuzzi P, Marasà L, Cappello F, Zumbo G, Farina F. Isolation and characterization of Oct-4+/HLA-G+ mesenchymal stem cells from human umbilical cord matrix: differentiation potential and detection of new markers. *Histochem Cell Biol.* 2009; 131(2):267-282.
67. Präbst K, Engelhardt H, Ringeler S, Hübner H. Basic Colorimetric Proliferation Assays: MTT, WST, and Resazurin. *Methods Mol Biol.* 2017; 1601:1-17.
68. Rinaldi S, Maioli M, Santaniello S, Castagna A, Pigliaru G, Gualini S, Margotti ML, Carta A, Fontani V, Ventura C. Regenerative treatment using a radioelectric asymmetric conveyor as a novel tool in antiaging medicine: an in vitro beta-galactosidase study. *Clin Interv Aging.* 2012; 7:191-194.
69. Casadei R, Piovesan A, Vitale L, Facchin F, Pelleri MC, Canaider S, Bianconi E, Frabetti F, Strippoli P. Genome-scale analysis of human mRNA 5' coding sequences based on expressed sequence tag (EST) database. *Genomics.* 2012; 100(2):125-130.
70. Facchin F, Vitale L, Bianconi E, Piva F, Frabetti F, Strippoli P, Casadei R, Pelleri MC, Piovesan A, Canaider S. Complexity of bidirectional transcription and alternative splicing at human RCAN3 locus. *PLoS One.* 2011; 6:e24508.
71. Beraudi A, Bianconi E, Catalani S, Canaider S, De Pasquale D, Apostoli P, Bordini B, Stea S, Toni A, Facchin F. In vivo response of heme-oxygenase-1 to metal ions released from metal-on-metal hip prostheses. *Mol Med Res.* 2016; 14(1):474-480.
72. Bustin SA, Benes V, Garson JA, Hellemans J, Huggett J, Kubista M, Mueller R, Nolan T, Pfaffl MW, Shipley GL, Vandesompele J, Wittwer CT. The MIQE

- guidelines: Minimum information for publication of quantitative real-time PCR experiments. *Clin Chem.* 2009; 55(4):611-622.
73. Maioli M, Rinaldi S, Santaniello S, Castagna A, Pigliaru G, Delitala A, Lotti Margotti M, Bagella L, Fontani V, Ventura C. Anti-senescence efficacy of radio-electric asymmetric conveyer technology. *Age (Dordr).* 2014; 36(1):9-20.
 74. Carvalho MM, Teixeira FG, Reis RL, Sousa N, Salgado AJ. Mesenchymal stem cells in the umbilical cord: phenotypic characterization, secretome and applications in central nervous system regenerative medicine. *Curr Stem Cell Res Ther.* 2011; 6(3):221-228.
 75. Hass R, Kasper C, Böhm S, Jacobs R. Different populations and sources of human mesenchymal stem cells (MSC): A comparison of adult and neonatal tissue-derived MSC. *Cell Comm Signal.* 2011; 9:12.
 76. Chen QM. Replicative senescence and oxidant-induced premature senescence. Beyond the control of cell cycle checkpoints. *Ann NY Acad Sci.* 2000; 908:111-125.